IEEE P802.15
Wireless Personal Area Networks

Project	IEEE P802.15 Working Group for Wireless Personal Area Networks (WPANs)
Title	Proposal for TG7r1 High-rate PD Communications
Date Submitted	March 7, 2016
Source	Nan Chi (Fudan Univerisity) Voice: [ ] Junwen Zhang (Fudan University) Fax: [ ] Yiguang Wang (Fudan Univeristy) E-mail: [ ]
Re:	[If this is a proposed revision, cite the original document.] [If this is a response to a Call for Contributions, cite the name and date of the Call for Contributions to which this document responds, as well as the relevant item number in the Call for Contributions.] [Note: Contributions that are not responsive to this section of the template, and contributions which do not address the topic under which they are submitted, may be refused or consigned to the "General Contributions" area.]
Abstract	[This document describes a PHY and MAC proposal for High-rate PD communications addressing the requirements in the Technical Considerations Document.]
Purpose	[Proposal]
Notice	This document has been prepared to assist the IEEE P802.15. It is offered as a basis for discussion and is not binding on the contributing individual(s) or organization(s). The material in this document is subject to change in form and content after further study. The contributor(s) reserve(s) the right to add, amend or withdraw material contained herein.
Release	The contributor acknowledges and accepts that this contribution becomes the property of IEEE and may be made publicly available by P802.15.

List of contributors

Nan Chi, Fudan University

Junwen Zhang, Fudan University

Yiguang Wang, Fudan University

Jianyang Shi, Fudan University

1. Overview

2. Normative references

3. Definitions, acronyms and abbreviations

4. General description, network topologies

5. MAC

5.1. Duplex mode
5.2. Superframe
5.3. Peer-to-peer
5.3.1. VPAN establishment
5.3.2. Association and disassociation
5.3.3. Link maintainance
5.3.4. CSI feedback and link adaptation
5.3.5. Interference coordination
5.3.6. Acknowledgement and retransmission
5.4. Star
5.4.1. VPAN establishment
5.4.2. Association and disassociation
5.4.3. Link maintainance
5.4.4. CSI feedback and link adaptation
5.4.5. Interference coordination
5.4.6. Acknowledgement and retransmission
5.4.7. Mobility and handover
5.5. Relaying
5.6. Coordinated network
5.6.1. VPAN establishment
5.6.2. Association and disassociation
5.6.3. Link maintainance
5.6.4. CSI feedback and link adaptation
5.6.5. Interference coordination
5.6.6. Acknowledgement and retransmission
5.6.7. Mobility and handover
5.7. Heterogeneous Operation of different OWC PHY modes
5.8. MAC frame formats
5.9. Command frames
5.10. Primitives for data service
5.11. Primitives for management service

6. Generic PHY

6.1. Adaptive OFDM concept
6.2. Frame Structure
6.2.1. Preamble
6.2.2. Channel estimation
6.2.3. Header
6.2.4. Data
6.3. Waveform

The PHY layer uses the adaptive OFDM waveform in both link directions with following extensions:

1) Bit and power loading is used in adaptive OFDM signal generation to maximum the transmission capacity.

2) Single-carrier frequency division multiple access (SC-FDMA) can be an optional choice for uplink, due to its advantage to provide low a peak-to-average power ratio (PAPR) for the transmit waveform.

3) Asymmetrically clipped optical OFDM (ACO-OFDM) can be used to improve the power efficiency.

6.3.1. Adaptive OFDM signal generation

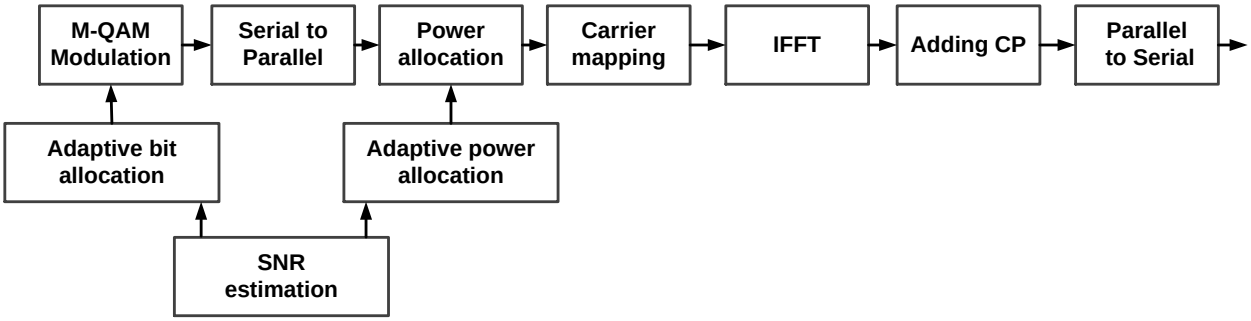

Fig. 1 adaptive OFDM signal generation

The adaptive OFDM signal generation implementing bit and power allocation is shown in Fig. 1 [1]. In the implementation, the OFDM transmitter consists of M-ary QAM modulation (M-QAM, 1 for BPSK, 2 for QPSK, 3 for 8-QAM, 4 for 16-QAM etc.) based on adaptive bit allocation, serial-to-parallel conversion, power allocation based on adaptive power allocation, carrier mapping, inverse fast Fourier transform (IFFT), adding cyclic prefix (CP) and parallel-to-serial conversion. Before applying bit and power allocation, the signal-to-noise ratio (SNR) of the channel is estimated through error vector magnitude (EVM) method:

$$EVM = \frac{\sum_{n=1}^{M} \left| S_n - S_{0,n} \right|^2}{\sum_{n=1}^{M} \left| S_{0,n} \right|^2} \quad , \; SNR = \frac{1}{EVM^2}$$

where S_n is the normalized nth measured symbol, $S_{0,n}$ is the ideal normalized constellation point of the nth symbol and N is the number of unique symbols in the constellation.

The total data rate can be calculated as

$$R = \frac{B(\sum_{k=1}^{N} \log_2 M_k)}{N}$$

where B is the modulation bandwidth, N is the total subcarrier number, and M_k is the constellation size of the kth subcarrier.

At the receiver side, the bit allocation information of every subcarrier is needed for M-QAM decoding.

6.3.2. Carrier mapping

Carrier mapping is performed for complex-to-real conversion, which can result in discrete multitone (DMT) signal. This is achieved by enforcing the following condition to OFDM signal:

$$x_{N-k} = x_k^*$$

Namely, the information symbols for the subcarriers k and N-k are complex conjugate to each other, and only half of the subcarriers are used for data.

6.3.3. IFFT

OFDM modulation can be implemented by using inverse discrete Fourier transform (IDFT).

$$X(k) = \frac{1}{N} \sum_{n=0}^{N-1} x_n e^{j2\pi nk/N}$$

where *k* denotes the sample index, x_n the complex-valued baseband signals in the frequency domain and N the block size of the IFFT.

6.3.4. Cyclic prefix

Cyclic prefix is used to resolve the channel dispersion-induced ISI and ICI. The CP insertion is a cyclic extension of the OFDM waveform into the guard interval, ΔG. The waveform in the guard interval is essentially an identical copy of that in the DFT window, with time shifted forward by t_s. The ISI-free OFDM transmission can be achieved when:

$$t_d < \Delta G$$

where t_d is the time delay between different OFDM subcarriers. The length of CP is determined by the symbol length and the time delay, which is variable. Typically the CP length is about 1/16 of a OFDM symbol.

6.3.5. Singlecarrier modulation (optional)

6.3.5.1 Single-carrier frequency division multiple access (SC-FDMA)

SC-FDMA can be an optional choice for uplink, due to its advantage to provide low a peak-to-average power ratio (PAPR) for the transmit waveform [2-3].

Similar to OFDM, SC-FDMA divides the transmission bandwidth into multiple parallel subcarriers maintaining the orthogonality of the subcarriers by the addition of the cyclic prefix (CP) as a guard interval. However, in SC-FDMA the data symbols are not directly assigned to each subcarrier independently like in OFDM. Instead, the signal which is assigned to each subcarrier is a linear combination of all modulated data symbols transmitted at the same time

instant. The difference of SC-FDMA transmission from the OFDM transmission which is an additional DFT block before the subcarrier mapping can be seen in Figure 2.

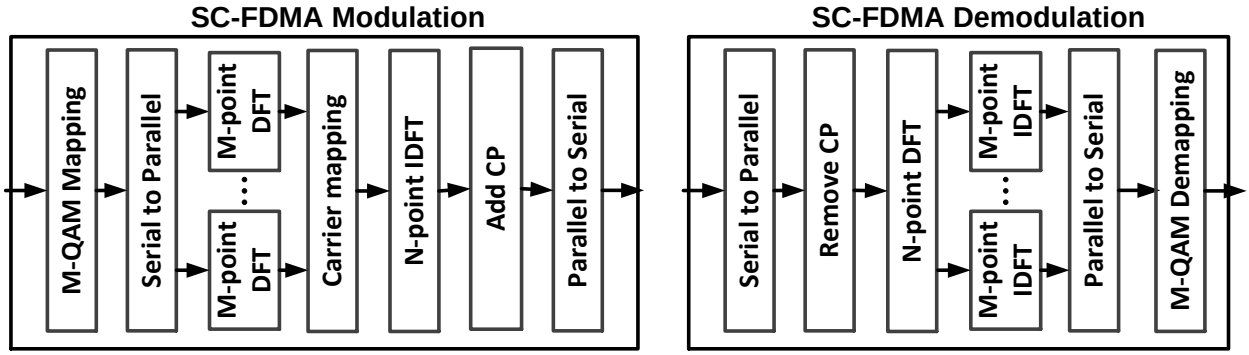

Fig. 2 the modulation and demodulation of SC-FDMA

At first, N points DFT is employed for each set. Then the baseband signal would be mapped from frequency domain into time domain through N points IDFT, which is similar to the conventional OFDM scheme.

6.3.5.2 Transform domain processing based channel estimation method for SC-FDMA [4]

Generally, the conventional TDA-based channel estimation method is employed for SC-FDMA systems. H(k) is calculated by averaging over multiple training symbols (TSs). In order to improve the accuracy of channel estimation and reduce the length of overhead, transform-domain processing (TDP) based method is proposed for channel estimation. Figure 3 shows the signal processing of TDP at the receiver.

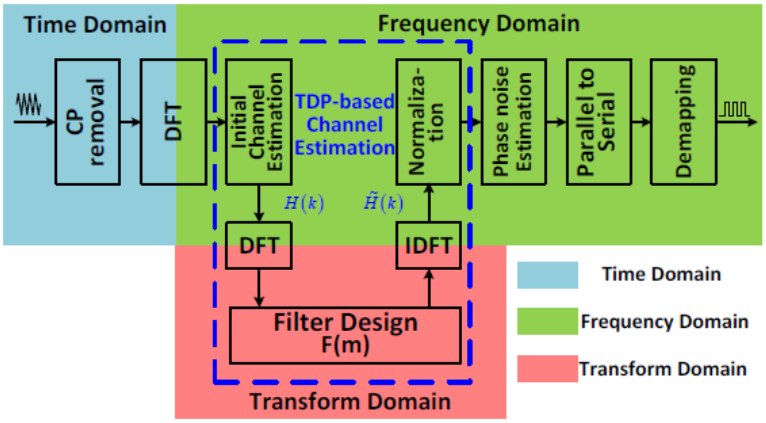

Fig. 3 the signal processing of TDP at the receiver

First, the transfer function H(k) is obtained through initial channel estimation. Then, H(k) is transformed to $H_T(m)$ by employing another discrete Fourier transform (DFT). $H_T(m)$ is in transform domain and expressed as

$$H_T(m) = \sum_{k=0}^{N-1} (H(k)) \cdot \exp(-j2\pi mk / N)$$

It's defined that the sequence in transform domain is the DFT of its counterpart in frequency domain. Because the transfer function is distorted by the high "frequency component" in

transform domain, a feasible way to improve the channel estimation is to employ a well-designed filter in transform domain. So an improved transfer function is given by

$$\tilde{H}(k)=\frac{1}{N}\sum_{m=0}^{N-1}H_T(m)\cdot F(m)\cdot\exp(j2\pi mk/N),\ F(m)=\begin{cases}1, & \frac{N}{2}-m_c<m<\frac{N}{2}+m_c\\ 0, & others\end{cases}$$

Here F(m) represents the transfer function of a designed filter and c_m is the cutoff coefficient which changes along with the channel parameters. The initial channel estimation could be operated by employing only one or several TSs, thus the overhead of OFDM signal can be reduced largely. On the other hand, the proposed method could reduce the noise out of the band in transform domain with appropriate filter, so the new transfer function $\tilde{H}(k)$ will be more accurate.

6.3.6. Unipolar modulation (optional)

The time domain OFDM signal envelope is utilized to modulate the intensity of the LED. So the signal needs to be non-negative, and a large DC bias has to be used to make OFDM signals non-negative, i.e. DC-biased OFDM (DCO-OFDM), which results in low power efficiency and low modulation depth. In order to overcome this disadvantage, asymmetrically-clipped optical OFDM (ACO-OFDM) can be used as a unipolar modulation scheme to improve the power efficiency [5].

For ACO-OFDM, the time domain signal is made unipolar by simply clipping the negative part at the zero level, which does not need a large DC bias. That is:

$$s(t)=\begin{cases}a(t), & a(t)\geq 0\\ 0, & a(t)<0\end{cases}$$

here a(t) is the generated bipolar OFDM signal, s(t) is the unipolar OFDM signal after clipping.

If only the odd subcarriers are modulated by signals, the effect of clipping is to reduce the amplitude of all the odd subcarriers by half and to cause intermodulation distortion which falls on the even subcarriers only. Thus the effect of clipping on the odd subcarriers is simply a multiplication of these components by a constant 0.5. Clipping does not result in inter-carrier interference (ICI) on the odd subcarriers, while even subcarriers are vacant. The diagram of ACO-OFDM modulation is shown in Figure 4.

Fig. 4 the diagram of ACO-OFDM modulation

Moreover, the advantages of ACO-OFDM is not only the higher power efficiency, but also the reduction of inter-carrier interference (ICI) caused by signal-signal beating noise. For DCO-OFDM, every subcarrier is modulated by signal. Therefore the beating noise will affect all the subcarriers and result in severe ICI. However, for ACO-OFDM, only odd subcarriers are modulated by signals while even subcarriers are vacant. So the beating noise from odd subcarriers will fall on even subcarriers and not affect the OFDM signals, which lead to the reduction of ICI caused by signal-signal beating noise, as shown in Figure 5.

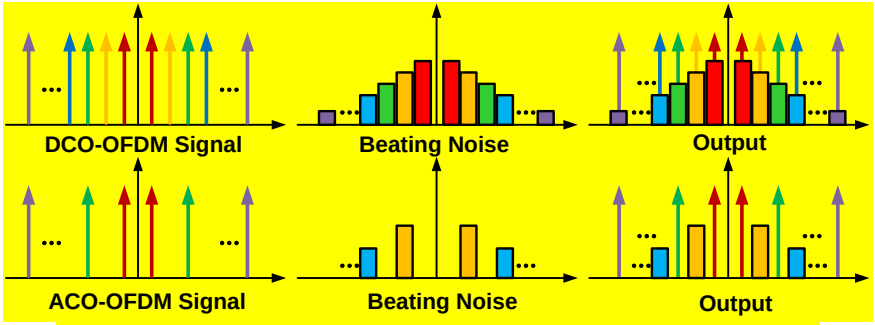

Fig. 5 the ICI comparison between DCO- and ACO-OFDM

6.3.7. Dimming

6.4. MIMO

MIMO allows the alignment required for such a interconnect to be achieved in the electronics as it is not necessary that light from a source precisely strikes a single detector. The motivation for using MIMO is therefore not only for capacity growth, but also to reduce the difficulties in achieving alignment physically by using electronic signal processing.

6.4.1. Modified frame structure

6.4.2. Reference symbols for MIMO channel estimation

The time-multiplexed training symbol (TS) based frequency domain equalization can be used for non-imaging MIMO channel estimation and de-multiplexing. The detail of the time-multiplexed TS is described in section 6.4.3.1.

6.4.3. MIMO transmission modes

6.4.3.1 Non-imaging MIMO transmission [6]

Light from each of the LED arrays is received by all the separate receivers, but with different strengths as shown in Figure 6. There are generally two types of propagation. Each LED has a line-of-sight (LOS) component that propagates to the receiver, and there is also a diffuse component to that propagates via reflections from the surfaces within the room.

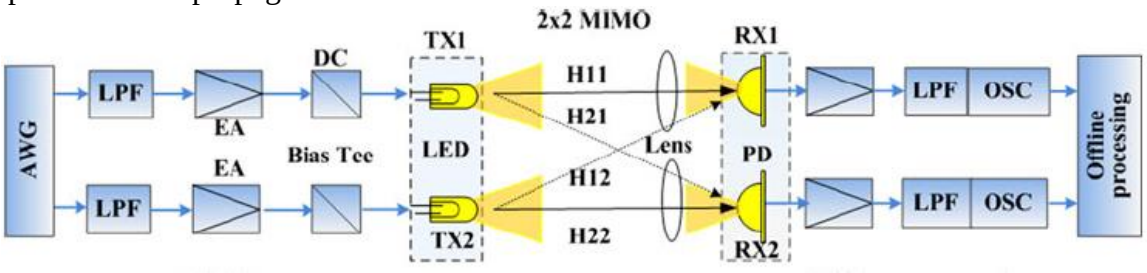

Fig. 6 the non-imaging MIMO

The non-imaging MIMO model can be expressed as:

$$\begin{pmatrix} Y_1 \\ Y_2 \end{pmatrix} = \begin{pmatrix} H_{11} & H_{12} \\ H_{21} & H_{22} \end{pmatrix} \cdot \begin{pmatrix} X_1 \\ X_2 \end{pmatrix} + \begin{pmatrix} N_1 \\ N_2 \end{pmatrix}$$

where $(Y_1\ Y_2)^T$ represent two received signals after free-space transmission, and $(X_1\ X_2)^T$ is the two independent signals at the TX, while $(N_1\ N_2)^T$ denote the system noise. The channel matrix elements $H_{i,j}$ (i = 1, 2; j = 1, 2) represent the gain from jth TX to ith RX.

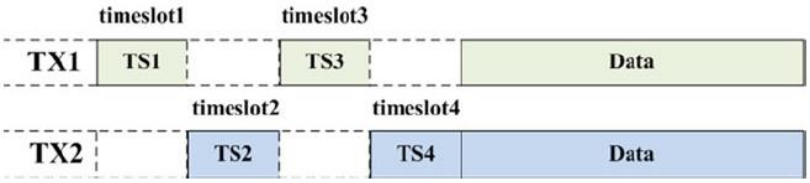

Fig. 7 Time-multiplexed training symbols for MIMO de-multiplexing

The time-multiplexed TS based frequency domain equalization can be used for MIMO channel estimation and de-multiplexing, as shown in Figure 7. Two pairs of TSs are transmitted in the front of signal to obtain the matrix for channel estimation and they can be expressed as

$$T_1 = \begin{pmatrix} TS_1 \\ 0 \end{pmatrix}, T_2 = \begin{pmatrix} 0 \\ TS_2 \end{pmatrix}$$

of which TS_1 and TS_2 are made up with binary phase shift keying signals inserted in front of two independent streams. Zero-forcing (ZF) and minimum-mean-square-error can be applied for MIMO processing. The obtained channel matrix can be expressed as:

$$H = \begin{pmatrix} H_{11} & H_{12} \\ H_{21} & H_{22} \end{pmatrix} = \begin{pmatrix} Y_{11}/TS_1 & Y_{12}/TS_2 \\ Y_{21}/\mathrm{TS}_1 & Y_{22}/TS_2 \end{pmatrix}$$

where Y_{11} and Y_{21} represent the received TS of the first symbol of RX1 and RX2, while Y_{12} and Y_{22} represent the received TS of the second symbol of RX1 and RX2, respectively. After obtaining the channel matrix H, the transmitted signal can be recovered by:

$$X_1 = (H_{22} * Y_1 - H_{12} * Y_2) / (H_{22} * H_{11} - H_{12} * H_{21})$$

$$X_2 = (H_{11} * Y_2 - H_{21} * Y_1) / (H_{22} * H_{11} - H_{12} * H_{21})$$

By using this method, the de-multiplexing and post-equalization can be simultaneously realized

6.4.3.2 Imaging MIMO transmission [7]

Imaging MIMO requires each LED array imaging onto a detector array, and the light propagates directly to the corresponding detector as shown in Figure 8. So the channel crosstalk can be neglected, and the channel matrix can be simplified and regarded as a diagonal matrix:

$$H = \begin{pmatrix} H_{11} & 0 \\ 0 & H_{22} \end{pmatrix} = \begin{pmatrix} Y_{11}/TS_1 & 0 \\ 0 & Y_{22}/TS_2 \end{pmatrix}$$

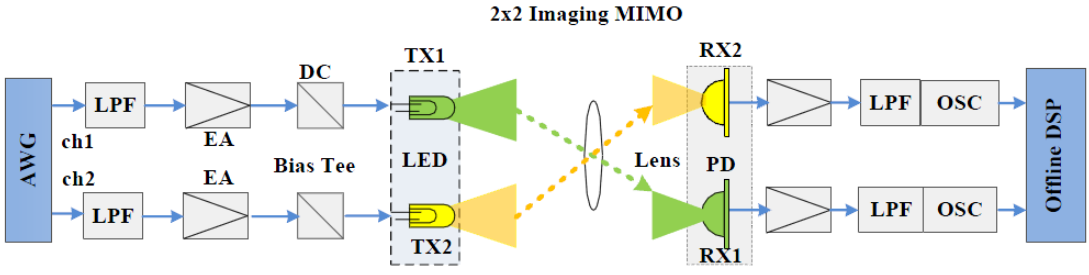

Fig. 8 the imaging MIMO

6.4.3.3. Polarization division multiplexing (PDM) VLC transmission [8]

Figure 9 shows a block diagram of this PDM VLC transmission. As the lights emitting from incoherent LEDs are natural lights all polarization directions are included and they can be decomposed as two orthogonal bases of x polarization and y polarization, respectively. A linear x-polarizer that can only allow components in the x polarization direction passing through is implemented at transmitter1 (TX1); meanwhile, a linear y polarizer that can only allow components in the y polarization direction passing through is employed at TX2. After passing through x-polarizer1and y-polarizer1, we can obtain linearly polarized light, but they will be mixed up after free-space transmission. At the receiver (RX), two corresponding polarizers should be implemented to filter out the unwanted polarized lights, thus obtaining the transmitting signals.

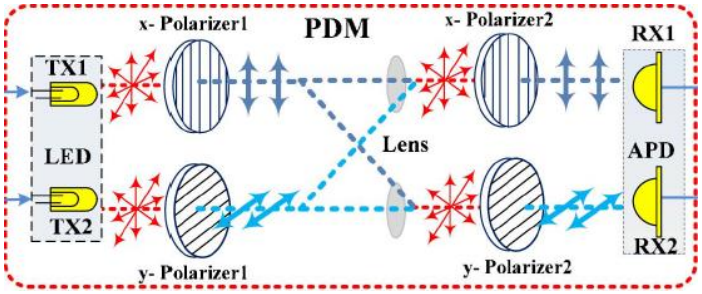

Fig. 9 the PDM VLC transmission

Assuming the offset angles between x-polarizer1 and x-polarizer2, x-polarizer1 and y-polarizer2, y-polarizer1 and x-polarizer2, and y-polarizer1 and y-polarizer2 are α_{11}, α_{12}, α_{21} and α_{22}, respectively, according to the Malus Law, the received optical intensity of each avalanche photodiode (APD) can be expressed as

$$\begin{pmatrix} Y_1 \\ Y_2 \end{pmatrix} = H \begin{pmatrix} I_1 \\ I_2 \end{pmatrix} + N = \frac{1}{2} \begin{pmatrix} \cos^2 \alpha_{11} & \cos^2 \alpha_{12} \\ \cos^2 \alpha_{21} & \cos^2 \alpha_{22} \end{pmatrix} \begin{pmatrix} I_1 \\ I_2 \end{pmatrix} + N$$

where Y_1 and Y_2 represent the received optical intensity of RX1 and RX2; meanwhile, I_1 and I_2 represent the emitted optical intensity from TX1 and TX2. H and N denote the channel matrix and noise.

6.5. Channel coding

6.5.1. Channel coding for the header

6.5.2. Channel coding for the data

6.5.3. Channel coding for MIMO

6.5.3.1 Self-adaptive space-time block coding (STBC) for MISO VLC transmission [9-10]

Space-time block coding (STBC) technique, one of representative multiple antenna techniques, can easily provide the diversity at receiver for MISO VLC transmission as shown in Figure 10.

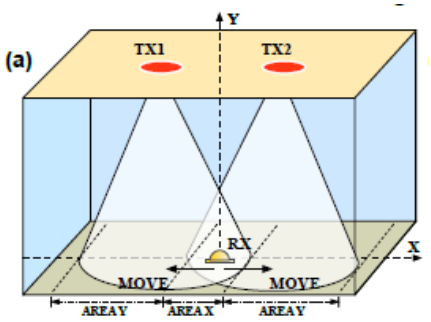

Fig. 10 the diagram of MISO VLC transmission

Alamouti's STBC scheme is employed to encode the data with two transmit LEDs and one receiver. And its space-time encoding can be described as follow:

$$\begin{bmatrix} c_1 & c_2 \\ -c_2^* & c_1^* \end{bmatrix}$$

Where c_1 and c_2 are complex signals to be transmitted and * denotes a conjugate operation. Rows indicate the slot times of transmission T_1 and T_2. Columns represent the transmit LEDs.

$$r_1 = h_1 c_1 + h_2 c_2 + \eta_1$$

$$r_2 = -h_1 c_2^* + h_2 c_1^* + \eta_2$$

Where h_1 and h_2 are channel responses for LED 1 and 2, respectively. η_1 and η_2 are noises at time T_1 and T_2. The signal vector can be rewritten as,

$$r = \begin{bmatrix} r_1 \\ r_2^* \end{bmatrix} = \begin{bmatrix} h_1 & h_2 \\ h_2^* & -h_1^* \end{bmatrix} \begin{bmatrix} c_1 \\ c_2 \end{bmatrix} + \begin{bmatrix} \eta_1 \\ \eta_2^* \end{bmatrix} = Hc + n$$

Therefore, the decoded signal can be obtained as

$$\tilde{r} = \tilde{H}^H r = \tilde{H}^H H c + \tilde{H}^H n$$

In the above equation, if the channel estimation is perfect, that means, $\tilde{h}_1 = h_1$ and $\tilde{h}_2 = h_2$, then:

$$\tilde{r} = \rho c + n'$$

with $H \cdot H^H = \rho I_{2\times 2}$ and $n' = H^H n$. Considering the noise, the final decoder will be described as follow

$$\hat{c} = \arg\min_{\hat{c}\in c} \left\| \tilde{r} - \rho \hat{c} \right\|^2$$

6.5.3.2 Maximal ratio combining (MRC) based receiver diversity [11-12]

Receiver diversity technology can provide array gain which allows a system with multiple receive antennas in a fading channel. In receiver diversity, the independent outputs of multiple receivers are combined to obtain a resultant signal that is then passed through a demodulator. Most combine techniques are linear: the output of the combiner is just a weighted sum of the different branches, as shown in Figure 11**.** Here r_i is the received electrical signal of the ith branch, N_i is the noise power spectral density (PSD) of the ith branch, and α_i is the weight of the ith branch.

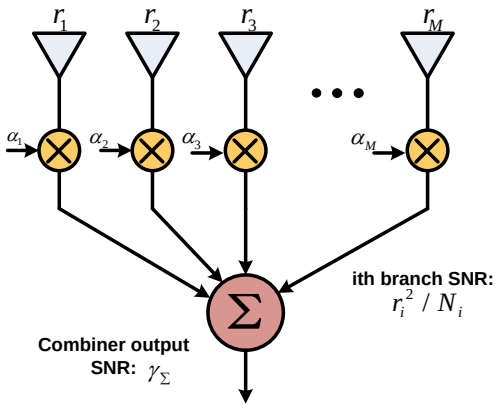

Fig. 11 the schematic diagram of MRC based receiver diversity

For receiver diversity, the output is the weighted sum of all the branches. Thus the combiner output of the signal will be $r = \sum_{i=1}^{M} \alpha_i r_i$. The total noise PSD at the combiner output will be $N_{tot} = \sum_{i=1}^{M} \alpha_i^2 N_i$. So the output SNR of the combiner is:

$$\gamma_\Sigma = \frac{r^2}{N_{tot}} = \frac{\left[\sum_{i=1}^{M} \alpha_i r_i\right]^2}{\sum_{i=1}^{M} \alpha_i^2 N_i}$$

The goal of MRC is to find the weight α_i to maximize the output SNR γ_Σ of the combiner. It can be found that the output SNR of the combiner cannot exceed the sum of the SNRs of each branch. On the other hand, if and only if $\alpha_i = r_i / N_i$, the resulting combiner SNR becomes:

$$\gamma_\Sigma = \sum_{i=1}^{M} r_i^2 / N_i = \sum_{i=1}^{M} \gamma_i$$

Thus, the SNR of the combiner output is the sum of SNRs in each branch. The average combiner SNR increases linearly with the number of diversity branches M.

6.6. Relaying
6.6.1. Modified frame structure
6.6.2. Amplify and Forward
6.6.3. Decode and Forward
6.7. Coordinated Network
6.7.1. Modified frame structure
6.7.2. Reference symbols for CO channel estimation
6.7.3. CO transmission modes
7. Numerology
7.1. Low-bandwidth PHY mode
7.2. High-bandwidth PHY mode

The numerology used in the high bandwidth mode is given in Table 1.

Light source	LED	LED	LED	LED

Bandwidth (MHz)	600	200	100	20
Sample rate (MS/s)	1000	400	200	50
Sample time (ns)	1	2.5	5	20
Carrier spacing (kHz)	195.32	195.32	195.32	195.32
Carriers in use	2850	950	450	90
IFFT size	4096	2048	1024	256
CP length	320, 160	128, 64	64, 32	16, 8
Symbol duration (us)	5.12			
Bits per carrier	1, 2, 3, 4, 5, 6, 7, 8, 9, 10, 11, 12			
Modulation formats	BPSK, M-QAM			
Peak rate (Mb/s)	5985	1995	945	189
Min. rate (Mb/s)	87	35	14	3

A Annex: Performance Evaluation Results
A.1. Simulation Framework
A.2. Peer-to-Peer
A.2.1 Adaptive OFDM
A.2.2 Singlecarrier transmission
A.2.3 Unipolar transmission
A.3. MIMO
A.3. Star
8.4. Relaying
8.5. Coordinated network

References

[1]. Xingxing Huang, Siyuan Chen, Zhixin Wang, Jianyang Shi, Yiguang Wang, Jiangnan Xiao and Nan Chi, "2.0-Gb/s visible light link based on adaptive bit allocation OFDM of a single phosphorescent white LED," IEEE Photonics Journal 7(5), October 2015.

[2]. L. Tao, Jianjun Yu, Q. Yang, M. Luo, Z. He, Y. Shao, J. Zhang, N. Chi, "Spectrally efficient localized carrier distribution scheme for multiple-user DFT-S OFDM RoF PON wireless access systems", Optics Express, Vol. 20, No. 28, pp. 29665-29672 (2012).

[3]. L. Tao, Jianjun Yu, Y. Fang, J. Zhang, Y. Shao, N. Chi, "Analysis of noise spread in optical DFT-S OFDM systems", J. of Lightwave Technol. Vol. 30, No. 20, pp. 3219-3225 (2012).

[4]. Li Tao, Jianjun Yu, Qi Yang, Yufeng Shao, Junwen Zhang, and Nan Chi,"A novel transform domain processing based channel estimation method for OFDM radio-over-fiber systems," [J] Opt. Express, Vol. 21, No. 6, pp. 7478-7487, (2013).

[5]. Yiguang Wang, Yuanquan Wang, and Nan Chi, "Experimental verification of performance improvement for a gigabit WDM visible light communication system utilizing asymmetrically clipped optical OFDM", Photonics Research, Vol. 2, No. 5, (2014).

[6]. Yuanquan Wang, and Nan Chi, "Demonstration of High-Speed 2×2 Non-Imaging MIMO Nyquist Single Carrier Visible Light Communication with Frequency Domain Equalization,"Journal of Lightwave Technology, Vol. 32, No. 11, 2014.

[7]. Yuanquan Wang, and Nan Chi, "Indoor Gigabit 2x2 Imaging Multiple-input Multiple-output Visible Light Communication," Chinese Optics Letters,Vol. 12 Issue 10, pp.100603- (2014).
[8]. Yuanquan Wang, Chao Yang, Yiguang Wang, and Nan Chi, "Gigabit polarization division multiplexing in visible light communication." Optics Letters 39(7), 1823-1826 (2014).
[9]. J. Shi, Y. Wang, X. Huang, et al. "Enhanced Performance employing STBC aided coding for LED based Multiple Input Single Output Visible Light Communication Network." Microwave and Optical Technology Letters, 2015, 57(12): 2943-2946.
[10]. J. Shi, X. Huang, Y. Wang, et al. "Improved Performance of a high speed 2×2 MIMO VLC network Based on EGC-STBC". ECOC 2015
[11]. Jiehui Li, Xingxing Huang, and Nan Chi, "Enhanced performance of single-input multiple-output visible light communication system utilizing space diversity technology," Optical Engineering, 54(3): 036109, 2015.
[12]. Yiguang Wang, X. Huang, Li Tao, and Nan Chi, "1.8-Gb/s WDM Visible Light Communication Over 50-meter Outdoor Free Space Transmission Employing CAP Modulation and Receiver Diversity Technology" OFC 2015, M2F. 2.